EasyChair Preprint

№ 815

Insights on the Effect of Ethanol on the Formation of Aromatics

Qi Wang and Angela Violi

March 6, 2019

INSIGHTS ON THE EFFECT OF ETHANOL ON THE FORMATION OF AROMATICS

Qi Wang[1] and Angela Violi[1,2]
avioli@umich.edu
1. Department of Mechanical Engineering, University of Michigan, 2350 Hayward St, Ann Arbor, MI 48109-2125, United States
2. Departments of Chemical Engineering, Biomedical Engineering, Macromolecular Science and Engineering, Biophysics Program, University of Michigan, Ann Arbor, MI, United States

Abstract
Polycyclic aromatic hydrocarbons (PAHs) and soot are generated by combustion processes, such as transportation, power generation, and waste incineration. Their escape from these processes into the atmosphere can cause both acute and long-term respiratory effects, and their deposition on soil and plants and in the surface water constitutes an important contamination of the human food chain. The addition of oxygenated compounds to hydrocarbon fuels have shown a reduction in PAHs, CO2, unburned hydrocarbons and soot. However, uncertainties still remain regarding the key reaction mechanisms responsible for these effects. In this paper, we report on the molecular mechanisms that contribute to the formation of polycyclic aromatic compounds in ethanol-doped ethylene flames, using a combination of deterministic and stochastic methods. Six ethylene/air premixed flame conditions with two equivalence ratios and two ethanol doping percentages were studied. Results show a reduction of acetylene, small aromatics, and large PAHs mole fractions when the percentage of added ethanol increases in ethylene flames. Stochastic modeling results then revealed the percentage of oxygenated species has a maximum of 45% at a HAB of 2 mm in all flames. Analysis of the formed oxygenated structures shows that most of them are phenols, around 15% are furans, and a small amount are ethers. In addition, results indicate a reduction in both chemical growth rate and cumulative chemical growth when increasing the ethanol doping percentage. This could further be accounted for the soot reduction with ethanol additions.

Introduction
Transportation is the largest consumer of petroleum-derived fuels in the world and the main emitter of atmospheric pollutants in urban centers (greater than 75%). Due to the growing energy demand, the severe air pollution issues in city centers, and the more restrictive environmental regulations to the road transport sector, there is an enormous need to develop and find alternative fuel sources and new technologies to reduce the vehicular emissions of air pollutants. Ethanol has attracted widespread interest because it is easily obtained from renewable resources (bioethanol) and because it can be used as a fuel extender for petroleum-derived fuels, as an oxygenate, as an octane enhancer, and as a pure fuel. Ethanol contains oxygen as part of its chemical strucutre , in addition to carbon and hydrogen, and the presence of oxygen-bonded atoms within the hydrocarbon structure may significantly change the main oxidation and molecular growth pathways. Indeed, reaction pathways not active during hydrocarbon combustion can be activated or enhanced by oxygen-borne atoms, leading to the formation of species with high molecular mass possibly still having oxygen atoms bonded to the structure.

There are many studies on how the doping of these oxygenates alters the chemistry of small gas-phase chemistry [1, 2, 3, 4], but less is known for the change in the large polycyclic aromatic compounds (PACs) that leads to incipient soot particles. Several recent papers [5, 6, 7] have revealed the importance of including oxygen chemistry of the PACs in order to explain the experimental observations. Elvati et al. [8, 7] indicated that the dimerization of PACs in general is more affected by the shape of the molecules rather than their masses. In addition, the authors reported that oxygenated species have less tendency to form dimers than pure hydrocarbons.

In this work, we report on our latest findings on the effect of ethanol addition to ethylene fuel on the formation and growth of aromatics in premixed flames. Six ethylene and ethanol-doped ethylene flames are analyzed using a combination of computational techniques. Growth mechanisms are characterized in terms of kinetic pathways at different locations in the flame and their relative importance is assessed at different stage along the combustion process in the flame.

Methodology

A combination of deterministic gas-phase and stochastic modeling was employed to study the effect of ethanol on the formation of aromatics.

Deterministic Model

Several previous studies have developed ethylene/ethanol flame combustion mechanisms. Wu et al. [9] used base mechanism from Howard and coworkers [10], and augmented the ethanol reactions from Marinov [11]. Gerasimov et al. [3] tested three mechanisms against experimental measurements: the first consists base mechanism from Frenklach and coworkers [12, 13] and the ethanol oxidation from Marinov [11]; the second includes the USC-Mech-II mechanism developed by Wang et al. [14] and again the ethanol oxidation from Marinov [11]; the last one is proposed by Konnov [15] which involves the reactions for ethanol. Elvati et al. [7] used a base mechanism developed by DAnna and Kent [16] and the ethanol oxidation from Marinov [11].

In this paper, the KAUST mechanism II (KM2) [17] with species up to coronene ($C_{24}H_{12}$) was merged with the ethanol oxidation from Sarathy et al. [18]. A total of 13 species and 111 reactions related to ethanol were merged with KM2 mechanism.

Validation of the gas-phase mechanism

In order to validate the new mechanism, we ran PREMIX code of the CHEMKIN [19] package with the merged mechanism and then compared with the gas-phase measurements by Gerasimov et al. [3]. Premixed atmospheric-pressure fuel-rich ethylene/oxygen/argon (pure) and ethylene/ethanol/oxygen/argon (doped) flames with the same equivalence ratio (ϕ = 1.7) were characterized experimentally. The pure flame has a mole fraction of $C_2H_4/O_2/Ar$ = 0.088/0.155/0.757, while the doped flame has a mole fraction of $C_2H_4/C_2H_5OH/O_2/Ar$ = 0.044/0.044/0.155/0.757, replacing 50% of ethylene with ethanol. The flow rates for both flames were maintained at 25.8 cm^3/s. The temperature profiles measured by experiments were input to the PREMIX code to minimize the uncertainty when modeling the heat loss with energy equations.

Gas-phase modeling

Studies show that the flame temperature generally decreases when increase the doping percentage of ethanol [20]. For example, Wu et al. [9] characterized six ethylene/air (pure) and

ethylene/ethanol/air (doped) flames experimentally with different equivalence ratio ($\phi = 2.34$ or 2.64) and doping percentage (0, 5 wt% and 10 wt%). The temperature profiles differ a lot among flames, thus the effect of temperature cannot be completely decoupled when studying the effect of doping ethanol. To isolate the effect of temperature, we modeled a set of flames using PREMIX code of the CHEMKIN [19] package by solving energy equations, similar to the approach by Golea et al. [4] when studying the effect ethanol doping on gas-phase species in benzene flames. We chose the base flame to be ethylene/air premixed flame with an equivalence ratio of 2.34 and mass flux of 7.82 mg/s cm^2 by Wu et al. [9]. We then applied the validated new mechanism to a set of ethylene/air (pure) and ethylene/ethanol/air (doped) flames with different equivalence ratio of 2.34 and 2,64, and doping percentage (molar basis) of 0, 20%, and 40%, using PREMIX code of the CHEMKIN [19] package by solving energy equation. The temperature profiles were kept nearly constant by adjusting the cold gas velocity.

Stochastic modeling

The gas-phase results from CHEMKIN were then input to a stochastoc modeling code to study the PACs formation mechanisms. The code, named Stochastic Nanopaticle Simulator (SNapS2) was developed by the Violi group, and has been validated with other systems [6, 7, 21, 22]. Its latest version utilizes kinetic Monte Carlo scheme and generic reactions depending on the chemical neighbourhoods (*i.e.*, sites). The SNapS2 code is able to generate particle time-history (*i.e.*, traces) given a initial molecule (*i.e.*, seed) and the gas-phase environment (*i.e.*, temperature and small gas-phase species mole fractions). When enough traces are sampled, a statistical distribution can be established for chemical and physical properties of the PACs. Compared with its previous version [21], the computational performance has been increased by two order of magnitudes and new oxygen chemistry such as furan rings formation [6] has been added to a mechanism with around 300 generic reactions.

To choose the seed molecules for the simulations, the small cyclic molecules with the highest mole fractions are chosen from the computed gas-phase profiles. Benzene, cyclopentadiene, and phenol were used as seeds for this modeling. They were weighed by the relative mole fractions at the starting location of each trace. A total of 32,000 traces were simulated for all six conditions.

Results and discussions

As first step in our study, we validated the new merged kinetic mechanism using experimental data collected in a premixed laminar flame by Gerasimov et al. Figure 1 shows the comparisons of modeling results and experimental measurements for both pure and doped flames.

The new mechanism predicts the fuel (C_2H_4 and C_2H_5OH) and oxidizer (O_2) mole fractions very well, both as trends and values. The mole fractions of the final combustion products (H_2O, CO, CO_2) also show great agreement between modeling and experimental results. While the new mechanism captures the peak of C_2H_2 mole fraction, the trend after the peak is not well-captured. However, this result is similar to the one shown by Gerasimov et al. [3] when using USC-Mech-II mechanism [14] coupled with ethanol oxidation from Marinov [11]. Since KM2 mechanism is using USC-Mech-II mechanism for species up to benzene, this result is reasonable.

To verify that the merged mechanism does not substantially change the base mechanism (KM2), simulations have been done with the base and merged mechanisms on the pure flame and only small differences could be be observed.

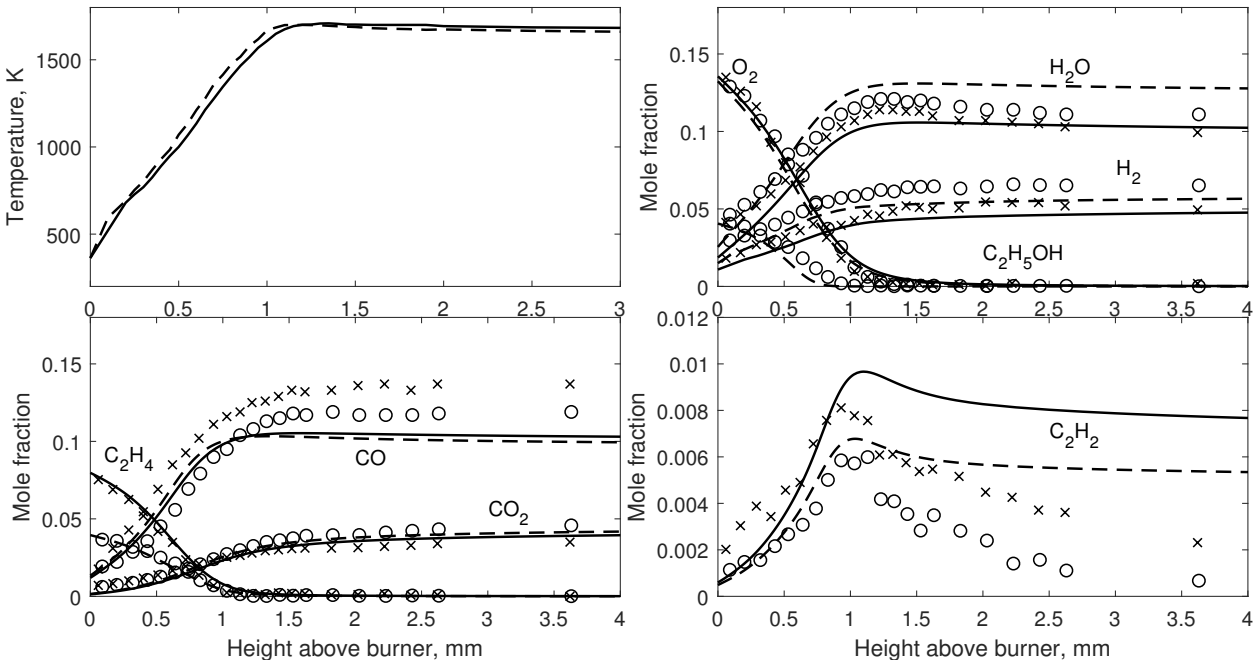

Figure 1: Comparison between experimentally measured temperature profile and selected species mole fractions and modeling results. Upper left is the experimentally measured temperature profile for pure (solid line) and doped (dash line) flame. The rest three sub-figures are mole fractions of O_2, H_2, H_2O, and C_2H_5OH (upper right); C_2H_4, CO, and CO_2 (lower left); and C_2H_2 (lower right) at different height above burner, for modeling results of pure flame (solid lines) and doped flame (dash lines), as well as experiment results for pure flame (cross) and doped flame (dots).

Figure 2 shows the mole fractions of gas-phase species C_6H_6, C_2H_2, H_2, and H_2O for all six flame conditions.

For pure flames, the one with higher equivalence ratio yields larger mole fractions of C_6H_6, C_2H_2, and H_2 as expected for a more sooting flame. Mole fractions of H_2O are almost the same for flames with two equivalence ratios. Within the same equivalence ratio, increasing ethanol doping percentage would result less C_2H_2 and C_6H_6, and more H_2 and H_2O. Reduction of C_2H_2 when doping ethanol is observed in several studies, and is considered to be one of the reasons for the soot formation decrease [1, 2, 9, 23, 24]. Reduction of C_6H_6, which is the dominating species for small aromatics, is studied by Wu et al. [9]. The increase in H_2O is also observed in other studies and considered to influence the soot formation by removal of H atoms through reaction $H_2O + H \longrightarrow OH + H_2$ [24].

Since KM2 mechanism has species with molecular masses up to coronene, the amounts of small aromatics (one to two rings) and large PAHs (three or more rings) were also analyzed from the gas-phase results. Figure 3 shows the results for small aromatics and large PAHs.

The mole fraction of small aromatics is dominated by benzene, thus the profile trends look very similar to the C_6H_6 profiles shown in Fig. 2. The small aromatics experiences a rapid growth after 2 mm where both H and C_2H_2 reach their peak values. The small aromatics start to decay after an HAB of 10 mm because of the gas-phase consumption to larger PAHs. The mole fraction of large PAHs is dominated by acenaphthylene (A2R5, $C_{12}H_8$), cyclopenta[cd]pyrene (A4R5, $C_{18}H_{10}$), and anthanthrene ($C_{22}H_{12}$), indicating a preference of forming 5-membered rings from modeling results [21]. Unlike small aromatics, the large PAHs

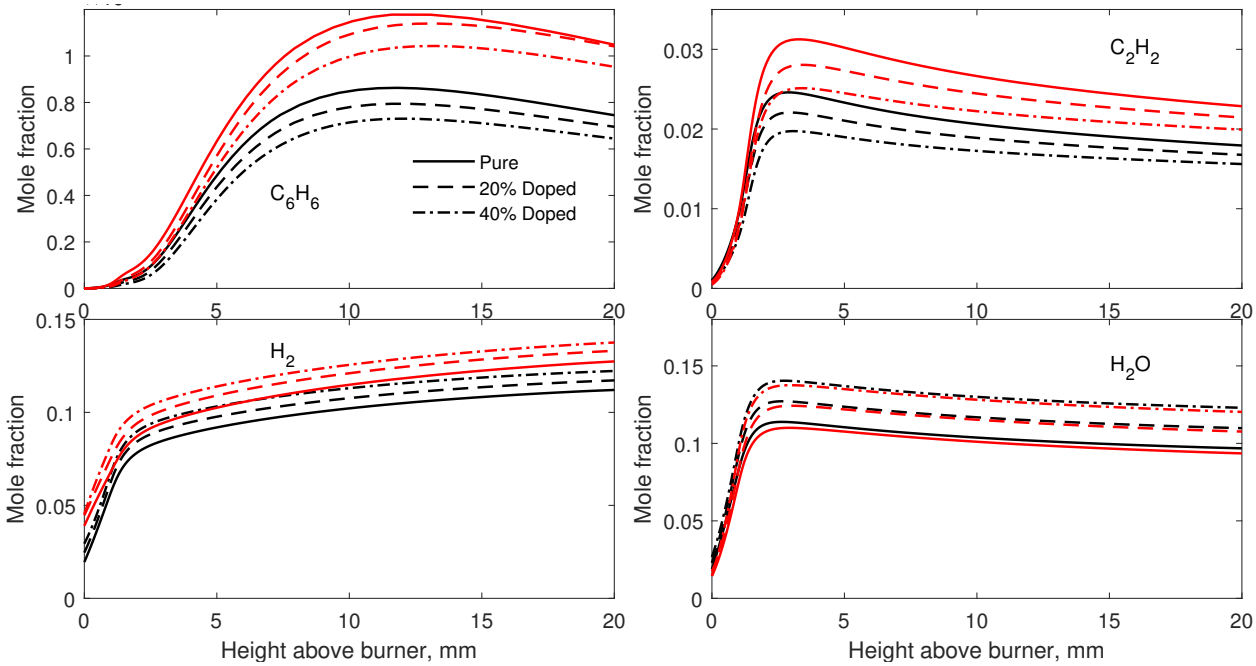

Figure 2: Selected species mole fractions from gas-phase modeling results. Four sub-figures are mole fractions of C_6H_6 (upper left), C_2H_2 (upper right), H_2 (lower left) and H_2O (lower right) from modeling results. Six lines represent pure flames (solid line), 20% doped flames (dashed line), and 40% doped flames (dash-dot line) with equivalence ratio of 2.34 (black) and 2.64 (red).

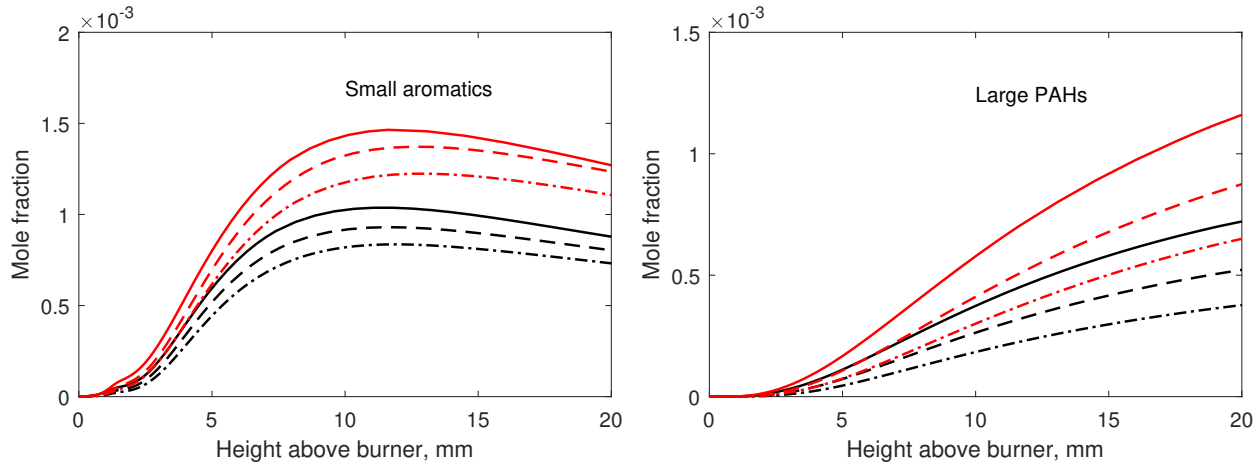

Figure 3: Mole fractions of small aromatics (one to two rings, left) and large PAHs (three or more rings, right) for all 6 flames from gas-phase modeling results. Six lines represent pure flames (solid line), 20% doped flames (dashed line), and 40% doped flames (dash-dot line) with equivalence ratio of 2.34 (black) and 2.64 (red).

steadily accumulate in the gas-phase. Indeed, the mole fraction for both small aromatics and large PAHs decay with an increase of ethanol doping percentage. A reduction of 20% and 50% of large PAHs is observed when doping 20% and 50% ethanol into ethylene/air premixed flames.

While gas-phase modeling can study the trends for some small aromatics and large PAHs, limited by the number of species, the vast diversity of the PACs cannot be studied within. SNapS2 provides information on the distributions of PACs' physical and chemical properties at different locations in the flames. From the SNapS2 results, while hydrogen-abstraction-acetylene(C_2H_2)-addition (HACA) mechanism [25, 26, 27, 28] dominates most part of the flame, oxygenated species were largely observed from SNapS2 simulation results around the location where O is peaked. Figure 4 shows the percentage of oxygenated species as a function of HAB for different flames.

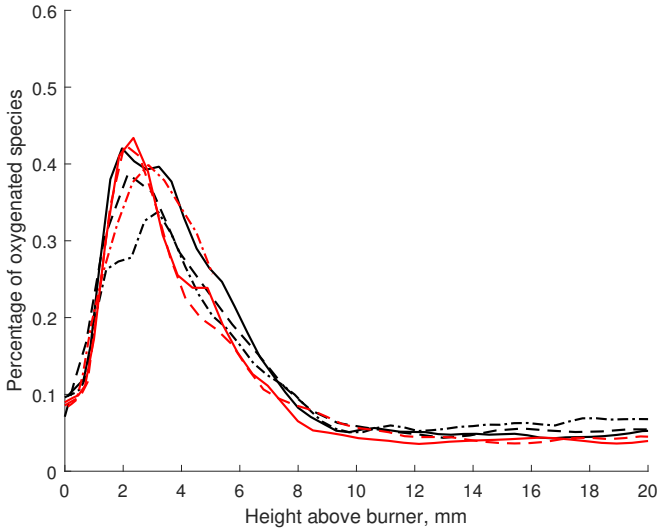

Figure 4: Percentage of oxygenated species in different flames as a function of HAB from SNapS2 modeling results. Six lines represent pure flames (solid line), 20% doped flames (dashed line), and 40% doped flames (dash-dot line) with equivalence ratio of 2.34 (black) and 2.64 (red).

The percentages of oxygenated species peak around 2 mm from the burner, which corresponds to the peak location of O and H mole fractions. The maximum value reaches 45% regardless of the flame, and then gradually decay to around 5% towards the end of the flame. Since our study isolates the effect of temperature, the O mole fraction profiles among the different flames are almost identical. Similar results have been shown by Golea et al. [4] in benzene premixed flames with the addition of ethanol. As indicated by several studies [6, 29], O mole fraction is critical for oxidation of the PAHs. The chain reactions for oxygenated species usually start by attaching O atom on aromatic sites of PAHs. Thus it is reasonable to have similar percentage of oxygenated species when the mole fractions of gas-phase oxidizing radicals are similar.

It is worth noticing that, doping ethanol would generally decrease the flame temperature [20] as previously discussed. This will then change the O profiles for pure and doped flames, as radical mole fractions are sensitive to temperature differences. Thus for cases where the effect of temperature cannot be decoupled, it is likely that the percentages of oxygenated species differ between pure and doped flames.

The mole fraction of C_2H_2 also peaks around the same location as O, which makes this environment ideal for the formation of furans [6]. Analysis of the formed oxygenated structures shows that most of them are phenols, around 15% are furans, and a small amount

are ethers. Interestingly, the formation and decay of the oxygen content happens frequently along a single trace identified by the SNapS code. Figure 5 shows the snapshots of three traces for the pure ethylene/air premixed flame with equivalence ratio 2.34.

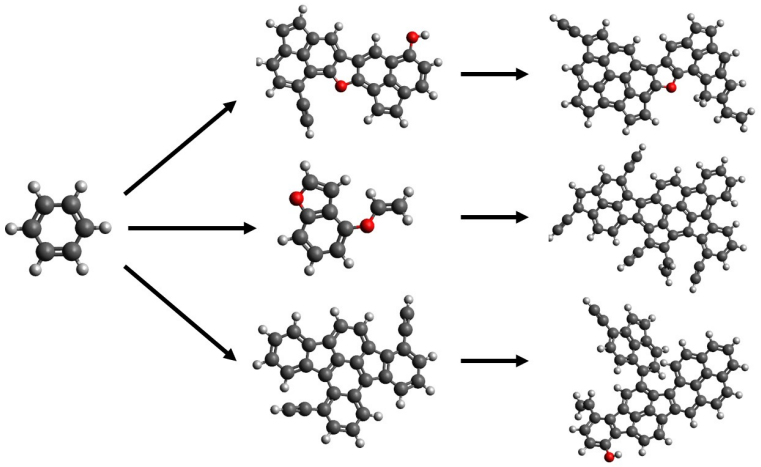

Figure 5: Snapshots of three traces for the pure ethylene/air premixed flame with equivalence ratio 2.34 using benzene as seed molecule. Atoms in dark, grey, and red correspond to carbon, hydrogen, and oxygen atoms. The molecules on the second and third column are extracted at an HAB of 2 mm and 10 mm respectively.

Some of the furan rings are preserved at high HAB (trace 1, upper), while others disappear (trace 2, middle). Formation of phenols and ethers are highly reversible at these conditions, thus the transformations between pure hydrocarbon and oxygenated-PACs happens quite often. Major reactions happening at different locations help better understand this phenomenon. Table 1 shows the top 5 reactions at HABs of 2 mm and 10 mm for the pure ethylene/air premixed flame with equivalence ratio of 2.34.

Statistical analysis of the reactions confirms the results discussed above. Oxygen chemistry dominates around HAB of 2 mm, while the major formation route for HACA is more relevant at 10 mm.

Finally, the PACs chemical growth rate for different flames shown in Fig. 6 is computed by averaging the molecular weights of different traces starting at the same location of the flame.

Indeed, we can see a significant reduction in both chemical growth rate and cumulative chemical growth of PACs over different HABs, when increasing the ethanol doping percentage. The peak of the growth rate again happens at a distance of 2 mm from the burner. The cumulative growth reaches a molecular mass of around 900 u for the pure flame. As shown by previous studies, the physical growth starts to be relevant at high molecular masses [8, 23, 30] (above 1000-1100 u). Thus the radical-radical recombination [31, 7] should be considered, which would significantly shift the molecular masses to higher ranges.

Conclusion

In this paper, we employed a combination of deterministic gas-phase and stochastic polycyclic-aromatic-hydrocarbons modeling methods to study the effect of ethanol additions on the formation of aromatics. After a newly merged gas-phase combustion mechanism with ethanol oxidation was validated against experimental measurements, six ethylene/air premixed flame conditions with two equivalence ratios and two ethanol doping percentages were then mod-

Generic Reaction	2mm	Generic Reaction	10mm
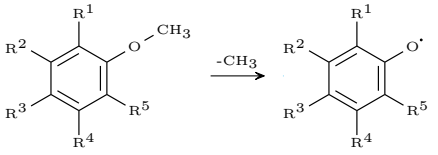	17.6%	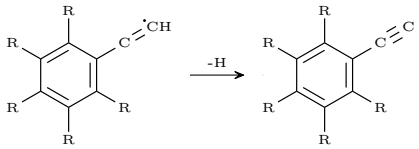	27.4%
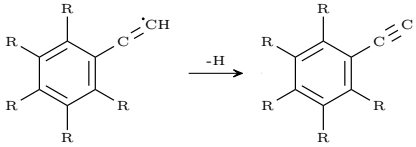	12.4%	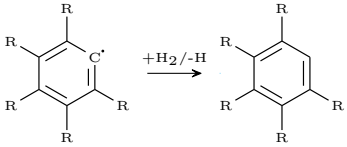	24.5%
	9.8%	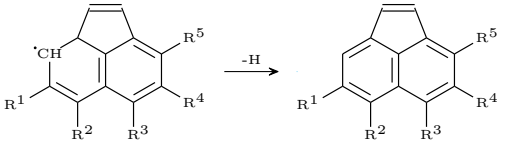	11.4%
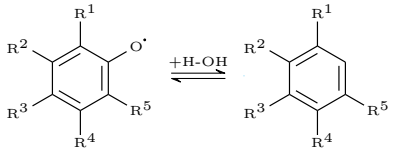	9.4%	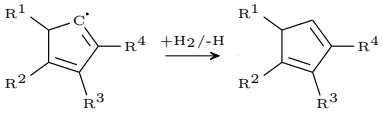	10.8%
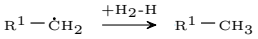	9.3%	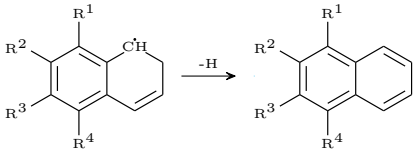	9.7%

Table 1: Top 5 reactions weighed by time from SNapS2-simulated traces for the pure ethylene/air premixed flame with equivalence ratio of 2.34, at a HAB of 2 mm and 10 mm.

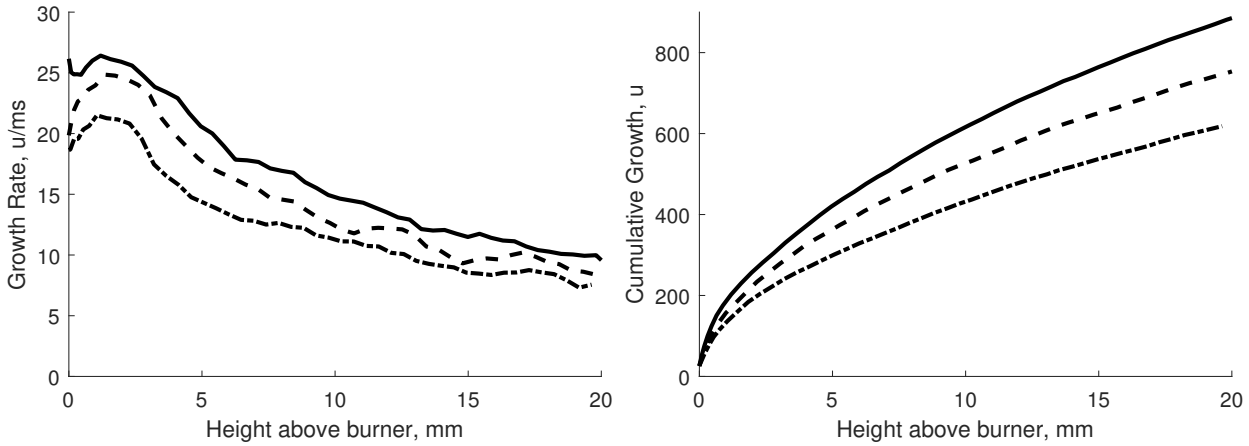

Figure 6: Chemical growth rate and cumulative chemical growth of PACs over different HAB by using benzene as starting molecule. Lines represent pure flames (solid line), 20% doped flames (dashed line), and 40% doped flames (dash-dot line) with equivalence ratio of 2.34.

eled. Gas-phase modeling results show a reduction of acetylene, small aromatics, and large PAHs mole fractions when increasing ethanol doping percentage in ethylene flames. Stochastic modeling results then revealed the percentage of oxygenated species has a maximum of 45% at a HAB of 2 mm among all flames. One possible reason is that we isolated the temperature effect in our study, resulted close O mole fraction profiles among all flames, thus observed similar oxygen chemistry among all flames. In addition, SNapS2 results indicate a reduction in both chemical growth rate and cumulative chemical growth when increasing the ethanol doping percentage. This could further be accounted for the soot reduction with ethanol additions.

*

References

[1] Inal, F., Senkan, S.M., "Effects of oxygenate additives on polycyclic aromatic hydrocarbons(pahs) and soot formation", *Combust. Sci. Technol.* 174:1–19 (2002).

[2] Leplat, N., Dagaut, P., Togb, C., Vandooren, J., "Numerical and experimental study of ethanol combustion and oxidation in laminar premixed flames and in jet-stirred reactor", *Combust. Flame* 158:705–725 (2011).

[3] Gerasimov, I.E., Knyazkov, D.A., Yakimov, S.A., Bolshova, T.A., Shmakov, A.G., Korobeinichev, O.P., "Structure of atmospheric-pressure fuel-rich premixed ethylene flame with and without ethanol", *Combust. Flame* 159:1840–1850 (2012).

[4] Golea, D., Rezgui, Y., Guemini, M., Hamdane, S., "Reduction of PAH and soot precursors in benzene flames by addition of ethanol", *J. Phys. Chem. A* 116:3625–3642 (2012).

[5] Skeen, S.A., Michelsen, H.A., Wilson, K.R., Popolan, D.M., Violi, A., Hansen, N., "Near-threshold photoionization mass spectra of combustion-generated high-molecular-weight soot precursors", *J. Aerosol Sci.* 58:86–102 (2013).

[6] Johansson, K.O., Dillstrom, T., Monti, M., El Gabaly, F., Campbell, M.F., Schrader, P.E., Popolan-Vaida, D.M., Richards-Henderson, N.K., Wilson, K.R., Violi, A., Michelsen, H.A., "Formation and emission of large furans and oxygenated hydrocarbons from flames", *Proc. Natl. Acad. Sci. U.S.A.* 113:8374–8379 (2016).

[7] Elvati, P., Dillstrom, V., Violi, A., "Oxygen driven soot formation", *Proc. Combust. Inst.* 36:825–832 (2017).

[8] Elvati, P., Violi, A., "Thermodynamics of poly-aromatic hydrocarbon clustering and the effects of substituted aliphatic chains", *Proc. Combust. Inst.* 34:1837–1843 (2013).

[9] Wu, J., Song, K.H., Litzinger, T., Lee, S.Y., Santoro, R., Linevsky, M., Colket, M., Liscinsky, D., "Reduction of PAH and soot in premixed ethyleneair flames by addition of ethanol", *Combust. Flame* 144:675–687 (2006).

[10] Richter, H., Granata, S., Green, W.H., Howard, J.B., "Detailed modeling of PAH and soot formation in a laminar premixed benzene/oxygen/argon low-pressure flame", *Proc. Combust. Inst.* 30:1397–1405 (2005).

[11] Marinov, N.M., "A detailed chemical kinetic model for high temperature ethanol oxidation", *Int. J. Chem. Kinet.* 31:183–220 (1999).

[12] Appel, J., Bockhorn, H., Frenklach, M., "Kinetic modeling of soot formation with detailed chemistry and physics: laminar premixed flames of C2 hydrocarbons", *Combust. Flame* 121:122–136 (2000).

[13] Wang, H., Frenklach, M., "A detailed kinetic modeling study of aromatics formation in laminar premixed acetylene and ethylene flames", *Combust. Flame* 110:173–221 (1997).

[14] Wang, H., You, X., Joshi, A.V., Davis, S.G., Laskin, A., Egolfopoulos, F., Law, C.K., "USC mech version II. high-temperature combustion reaction model of H2/CO/C1-C4 compounds", (2007), URL `http://ignis.usc.edu/USC_Mech_II.htm`.

[15] Konnov, A., "Implementation of the NCN pathway of prompt-NO formation in the detailed reaction mechanism", *Combust. Flame* 156:2093–2105 (2009).

[16] D'Anna, A., Kent, J., "A model of particulate and species formation applied to laminar, nonpremixed flames for three aliphatic-hydrocarbon fuels", *Combust. Flame* 152:573–587 (2008).

[17] Wang, Y., Raj, A., Chung, S.H., "A PAH growth mechanism and synergistic effect on PAH formation in counterflow diffusion flames", *Combust. Flame* 160:1667–1676 (2013).

[18] Sarathy, S.M., Kukkadapu, G., Mehl, M., Javed, T., Ahmed, A., Naser, N., Tekawade, A., Kosiba, G., AlAbbad, M., Singh, E., Park, S., Rashidi, M.A., Chung, S.H., Roberts, W.L., Oehlschlaeger, M.A., Sung, C.J., Farooq, A., "Compositional effects on the ignition of FACE gasolines", *Combust. Flame* 169:171–193 (2016).

[19] Reaction Design, *CHEMKIN-PRO 15112*, San Diego, 2011.

[20] Therrien, R.J., Ergut, A., Levendis, Y.A., Richter, H., Howard, J.B., Carlson, J.B., "Investigation of critical equivalence ratio and chemical speciation in flames of ethylbenzeneethanol blends", *Combust. Flame* 157:296–312 (2010).

[21] Lai, J.Y.W., Elvati, P., Violi, A., "Stochastic atomistic simulation of polycyclic aromatic hydrocarbon growth in combustion", *Phys. Chem. Chem. Phys.* 16:7969 (2014).

[22] Dillstrom, T., Violi, A., "The effect of reaction mechanisms on the formation of soot precursors in flames", *Combust. Theor. Model.* pp. 1–12 (2016).

[23] Frassoldati, A., Faravelli, T., Ranzi, E., Kohse-Hinghaus, K., Westmoreland, P.R., "Kinetic modeling study of ethanol and dimethyl ether addition to premixed low-pressure propeneoxygenargon flames", *Combust. Flame* 158:1264–1276 (2011).

[24] Salamanca, M., Sirignano, M., Commodo, M., Minutolo, P., DAnna, A., "The effect of ethanol on the particle size distributions in ethylene premixed flames", *Exp. Therm. Fluid Sci.* 43:71–75 (2012).

[25] Frenklach, M., Clary, D.W., Gardiner, W.C., Stein, S.E., "Detailed kinetic modeling of soot formation in shock-tube pyrolysis of acetylene", *Proc. Combust. Inst.* 20:887–901 (1985).

[26] Frenklach, M., Wang, H., "Detailed modeling of soot particle nucleation and growth", *Proc. Combust. Inst.* 23:1559–1566 (1991).

[27] Frenklach, M., "Reaction mechanism of soot formation in flames", *Phys. Chem. Chem. Phys.* 4:2028–2037 (2002).

[28] Frenklach, M., Schuetz, C.A., Ping, J., "Migration mechanism of aromatic-edge growth", *Proc. Combust. Inst.* 30:1389–1396 (2005).

[29] Frenklach, M., Liu, Z., Singh, R.I., Galimova, G.R., Azyazov, V.N., Mebel, A.M., "Detailed, sterically-resolved modeling of soot oxidation: Role of O atoms, interplay with particle nanostructure, and emergence of inner particle burning", *Combust. Flame* 188:284–306 (2018).

[30] DAnna, A., "Combustion-formed nanoparticles", *Proc. Combust. Inst.* 32:593–613 (2009).

[31] Johansson, K.O., Dillstrom, T., Elvati, P., Campbell, M.F., Schrader, P.E., Popolan-Vaida, D.M., Richards-Henderson, N.K., Wilson, K.R., Violi, A., Michelsen, H.A., "Radicalradical reactions, pyrene nucleation, and incipient soot formation in combustion", *Proc. Combust. Inst.* 36:799–806 (2017).